UDC 654.165
doi:10.15217/issn1684-8853.2018.1.85

PREDICTION OF OPERATIONAL PARAMETERS OF RADIO SIGNALS PASSING A LAND-SATELLITE LINK THROUGH STORMTIME IONOSPHERE

N. S. Blaunstein[a], *Dr. Sc., Phys.-Math., Professor, nathan.blaunstein@hotmail.com*
Y. Ben-Shimol[a], *PhD, Electrical Engineering, Senior Lecturer, benshimo@bgu.ac.il*
[a]*Ben-Gurion University of the Negev, P.O.B. 653, 1, Ben-Gurion St., Beer-Sheva, 74105, Israel*

Introduction: *The subject of this research became important during the recent decades due to the increasing demand in globalization of wireless networks by using long-path ionospheric radiowave propagation in land-satellite communication links.* ***Purpose:*** *Analyzing the key parameters of VHF/UHF radio waves in a satellite-land link which determine the fading effects occurring in storm-time mid-latitude ionosphere.* ***Results:*** *For perturbed plasma parameters experimentally caused by a magnetic storm, the absorption and phase fluctuations of the radio signals were examined. The scintillation index corresponding to signal scintillations in multi-path ionospheric communication links with fading was studied on the base of experimental data. It has been shown that ~10% density irregularities in the storm-time F region yield strong fast fading of radio signals in VHF/UHF frequency band with considerable signal intensity fluctuations (up to 1%) and phase deviations (up to hundreds of radians).* ***Practical relevance:*** *The obtained results allow you to predict multiplicative fading in ionospheric sub-channels and its impact on the total link budget in a full land-satellite communication link.*

Keywords *— Ionospheric Sub-Channel, Ionospheric Plasma Density Irregularities, Signal Intensity Scintillation Index, Amplitude Attenuation, Phase Fluctuation, Root Mean Square, VHF/UHF-Band Radio Waves.*

Citation: Blaunstein N., Ben-Shimol Y. Prediction of Operational Parameters of Radio Signals Passing a Land-Satellite Link through Stormtime Ionosphere. *Informatsionno-upravliaiushchie sistemy* [Information and Control Systems], 2018, no. 1, pp. 85–95. doi:10.15217/issn1684-8853.2018.1.85

Introduction

The ionosphere is one of the sub-channel (additional to the terrestrial and atmospheric sub-channels) of the global (e. g., mega-cell) land-satellite and transionospheric communication systems. It is well known that ionospheric irregularities cause strong fluctuations of the amplitude and phase of radio signals, i.e. fast fading. Enhanced irregularities are usually observed during magnetically disturbed periods, especially in the auroral ionosphere (see [1–9] and bibliography there). As the auroral boundary shifts equatorward during magnetic disturbances, it is usually assumed that mid-latitude scintillation events occur inside the expanded auroral zone. As was expected by many researchers dealing with satellite observations of the perturbed stormtime ionosphere, this phenomenon occurs not only in the proximity of the polar and auroral zones, but also in the sub-auroral and middle-latitude ionosphere [10–14]. This event occurs in about 15–17 % of time per year and usually is observed during several-day to several-week periods. It was found that during magnetic storms strong phase and amplitude scintillations (the scintillation index $S_4 \geq 0.5$) of radio signals of the satellite operating at 250 MHz [2] and 1.5 GHz [3] are observed (namely, near Boston, MA, USA and Ithaca, NY, USA) well equatorward of the auroral zone, up to the sub-auroral and mid-latitude ionosphere. Satellite and radar observations in the stormtime sub-auroral ionosphere [4–7] revealed irregular structures embedded within fast westward streams, called sub-auroral polarization streams (SAPS) [8]. In particular, strongly irregular plasma density structures are embedded within SAPS wave-like structures (called SAPSWS) [6, 7]. Thus, the Defense Meteorological Satellite Program (DMSP) for satellite observations, which coincided with the [2, 3] scintillation events, revealed SAPSWS-related irregular density troughs. Within the troughs, power spectral densities (PSD) ($\delta n_k = 10$–20 % with respect to non-disturbed ionospheric plasma n_0 [9]) of plasma irregularities (electron and ions, since plasma is quasi-neutral) in the range of apparent wave numbers from $k = 2\pi/\lambda = 0.85$ km^{-1} to $k = 12$ km^{-1}, λ is the wavelength, were well-approximated by a plasma density power-law $(\delta n_k/n_0)^2 k^{-p}$ with the spectral index of $5/3 < p \leq 2$ [9].

The spectral properties of plasma perturbations allow for predicting spectral characteristics of the radio signal with data (called the bandpass signal [15]), and finally predict the type of signal fading, flat or frequency selective, in such a perturbed ionospheric channel. These aspects are very actual for advanced wireless networks design based on modern techniques of signal processing, namely, orthogonal frequency division multiplexing (OFDM),

where each subscriber obtained very narrow bandwidth. The main goal of such a technique is to eliminate effects of the noise caused by multipath phenomena occurring in the channel with fading and by inter-subscriber interference [16]. Therefore, it is important to predict *a-priory* the type of the channel, frequency or time dispersive (or both), and to estimate the coherent bandwidth and time of coherency of such a channel with fading for the future performance of OFDM access technique [16]. Above example shows the actuality of this paper and research carried out in it.

This work describes fading phenomena and their effects on key parameters of radio signals in the land-satellite communication link passing through the structured storm-induced plasma region, filled by the "typical" small- and moderate-scale irregularities. The basic effects of irregular plasma structures, embedded within SAPS, on radio signals propagation via the perturbed stormtime ionosphere are briefly discussed in the first Section. In the Section following it presents the results of computation of signal integral absorption, amplitude and phase "point-to-point" deviations, and variations in the intensity and phase of radio signals propagating through this SAPSWS-related "typical" link. These results help to understand the fading phenomena effects for signals passing multipath ionospheric links during magnetic storms. Then, we conclude main effects of radio signals of various frequency bands occurring in the perturbed ionosphere during magnetic storms.

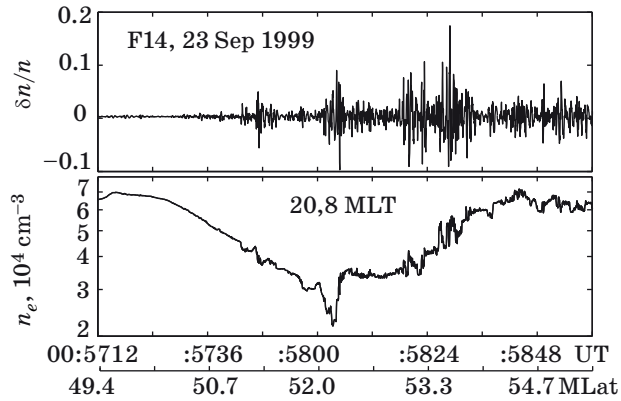

■ ***Fig. 1.*** DMSP F14 observations during the 23 September 1999 magnetic storm near Boston, MA, USA: (top) waveform of relative density variations $\delta n/n$ and (bottom) the density variation along the satellite track

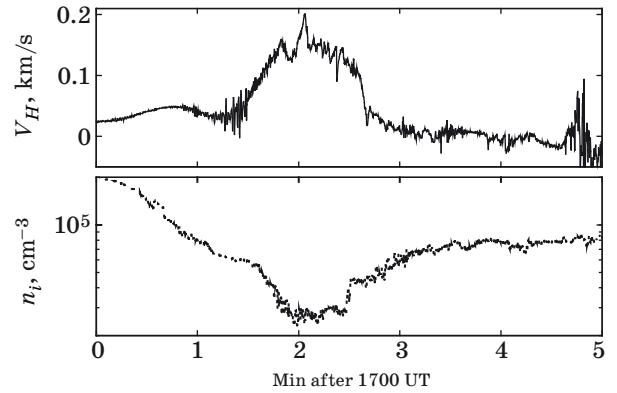

■ ***Fig. 2.*** (top) Horizontal (positive westward) component V_H of the convection velocity and (bottom) the plasma density from the DMSP F15 satellite on March 31, 2001 (extracted from [3])

Satellite Observations of Stormtime SAPS-related Density Irregularities

We start our discussions with analysis of several satellite campaigns carried out during period from the end of 20 century to beginning of 21 century. Thus, Fig. 1 (rearranged from [9]) shows a snapshot of plasma observations from the DMSP F14 satellite near the scintillation event near Boston, MA, USA during the 23 September 1999 magnetic storm [2]. Shown in the bottom panel is the plasma density variation along the satellite track measured by a spherical Langmuir probe sampled at the rate of 24 Hz. A detailed description of the probe and the whole DMSP/SSIES (Special Sensor for Ions, Electrons, and Scintillations) suite can be found in [10–13]. The top panel shows the corresponding waveform of plasma density deviations, $\delta n/n_0$, obtained applying 0.1–9.5 Hz bandpass elliptic filter (see details in [2]). Here δn is the perturbation of the background ionospheric non-disturbed plasma density (denoted by n_0). One can see also that enhanced density irregularities were present well equatorward of the boundary of auroral zone indicated by the vertical dashed line (i.e., beyond this zone the sub-auroral inonosphere is seen to be also perturbed).

We present now another example of stormtime sub-aurora density irregularities observed by the DMSP F13 and F15 satellites during the major magnetic storm of March 31, 2001 [3]. Fig. 2 shows a 5-min snapshot of the horizontal (positive westward) component of the convection velocity V_H (the top panel) and plasma density n_i (bottom) from F15/SSIES obtained by the ion drift meter and Langmuir probe sampled at the rates of 6 and 24 Hz, respectively.

Note that quite similar SAPS/trough patterns were observed throughout the storm also by the DMSP F13 satellite. As in [2, 3, 9, 10], we obtained the density waveforms in the SAPS regions applying 0.1–9.5 Hz bandpass elliptic filter. Their PSD are shown in Fig. 3 as a function of apparent frequencies. Likewise [9, 10], PSD is well represented by the law $\delta n_k/n_0 \sim k^{-p}$, $p = 2$ (or $\delta n_f/n_0 \sim f^{-2}$), where $k = 2\pi f/c$, and p is parameter of PSD [2–9].

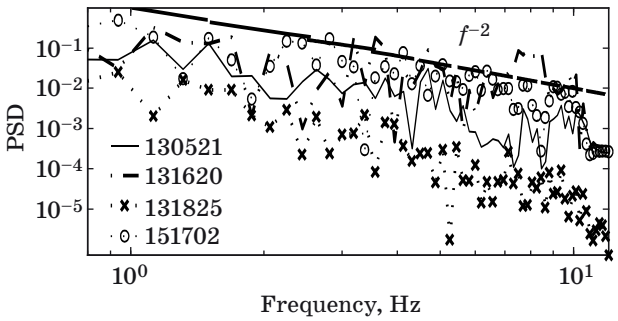

■ ***Fig. 3.*** Power spectral densities of plasma irregularities vs. the apparent frequency from the DMSP satellites and near the times designated in label: e. g., 130521 stand for the satellite F13 at 0521 UT (extracted from [9])

We emphasize that spatial and temporal variations cannot be separated in data from a single spacecraft and thus frequencies (wavelengths) mean apparent frequencies (scale-lengths). Given the satellite speed $v_s = 7.5$ km/s, apparent frequencies 1–10 Hz correspond to wavelengths $\lambda_s = 2\pi/k_s = v_s/f = 7.5–0.75$ km along the satellite track. Note also that after about 1900 UT short-scale oscillations faded away, whereas "smooth" SAPS/trough plasma structures remained throughout and even after the storm recovery phase. Such behavior is typical of SAPSWS that develop within 10–20 min and decay is ~1 hour after substorm expansion onsets [6, 7, 9].

Prediction of Main Parameters of Signals Passing Stormtime Perturbed Ionosphere

Main Parameters of the Radio Channel

In predicting the key parameters of radio signals passing through irregular ionosphere characterized by a spectral index $p = 1 + <n>$ ($<n>$ is the mean value of the plasma refractive index) or by the PSD index $p' = p - 2$ [15–21] it is important to show that the signal intensity fluctuations at a given frequency can be described by the Ricean K-parameter as a ratio of coherent and incoherent components of the total signal intensity [22]:

$$K = \langle I_{co}\rangle / \langle I_{inc}\rangle. \qquad (1)$$

Here $\langle I_{co}\rangle$ is the line-of-sight (LOS) component of the signal (called also the coherent part [14, 15, 22]) and $\langle I_{inc}\rangle$ is the incoherent component of the total signal intensity:

$$\langle I\rangle = \langle I_{co}\rangle + \langle I_{inc}\rangle, \qquad (2a)$$

where

$$\langle I_{inc}\rangle = \langle I_{co}\rangle \sqrt{\sigma_I^2}. \qquad (2b)$$

The scintillation index

$$\sigma_I^2 = \frac{\langle I^2\rangle - \langle I\rangle^2}{\langle I\rangle^2} = \frac{\langle I^2\rangle}{\langle I\rangle^2} - 1 \qquad (2c)$$

denoted in [1–9] as S_4, defines the normalized intensity of the signal fast fading.

For Gaussian zero-mean random signal amplitudes, the relationship between K and σ_I^2 (denoted in experimental works [1–5] as S_4) is simply

$$K^2 = 1/\sigma_I^2 \equiv 1/S_4. \qquad (3)$$

We note, according to [15] that for Gaussian nonzero-mean random signal amplitude distribution, as clear seen from relations (1)–(2c), formula (3) becomes more complicated. However, as was shown by many researchers investigating stochastic processes occurring in the perturbed ionosphere [15, 16–21, 23–36], the spatial distribution of ionospheric irregularities of natural and artificial nature can be correctly described by *zero-mean Gaussian law*, which according to ergodic theorem leads to the same Gaussian distribution of scattered radio signals in the time domain.

The basic characteristics of signal fading are derived by means of the approach developed in [16–20, 23–32] and summarized in [15, 21]. They are: 1) mean square phase fluctuation $\langle(\Delta\Phi)^2\rangle$; 2) outer scale L_0 of the disturbed ionospheric plasma structure; 3) inner scale l_0 of the plasma density irregularities.

In addition, to describe radio wave propagation in irregular plasmas, the outer scale L_0 should be compared with the Fresnel scale $d_F = \sqrt{\lambda Z_0}$ [15]. Here λ is the signal wavelength and Z_0 is the distance from the ionospheric layer filled by plasma inhomogeneities to the ground reception plane [15, 25–27]).

The spectrum of the signal intensity fluctuations can be derived via $\sqrt{\langle(\Delta\Phi)^2\rangle}$ [16–19, 21, 23, 30, 32, 34–36] by assuming that the root mean square (RMS) of phase fluctuations is larger than one radian. Moreover, in [15, 18, 19, 21, 30] have shown theoretically that at $k >> 1/L_0$ the power spectrum of phase fluctuations $S(k)$ in the perturbed inhomogeneous ionosphere is proportional to k^{-p} (e. g., f^{-p}), where $p = 2$ (see Fig. 3). This condition was proved by numerous observations of perturbed stormtime ionosphere (see [9, 21] and bibliography there).

Main Characteristics of the Radio Signal Fading

We analyze now propagation characteristics of the radio signal passing disturbed ionospheric region perturbed by geomagnetic storm. As it follows

from experimental data presented above, the background ionospheric plasma can be perturbed essentially in period of magnetic storm preparation. During this period the observed deviations of plasma density around its non-disturbed background can achieve 10–20 % (see Figs. 1, 2). There are several features should be estimated for predicting fading phenomena in the satellite communication links passing through the perturbed ionosphere, such as absorption, point-to point attenuation and phase deviation of radio signal amplitude along the radio path, as well as scattering phenomena caused signal intensity and random phase variations.

Absorption of Radio Signal in the Disturbed Ionosphere

To estimate losses due to absorption, i.e., the part of energy of radio signal, which is absorbed in the perturbed region of the ionosphere, from *D* to *F*, we propose here, following [15, 21, 35], to use a special value of absorption in decibels:

$$A_{\omega} = 10\log\frac{I_0}{I} \approx$$

$$\approx \frac{4.3}{c}\int \frac{\omega_{pe}^2(\nu_{em}+\nu_{ei}+\nu_{ee})}{[\omega^2+(\nu_{em}+\nu_{ei}+\nu_{ee})^2]}\,ds\ [\text{dB}], \qquad (4)$$

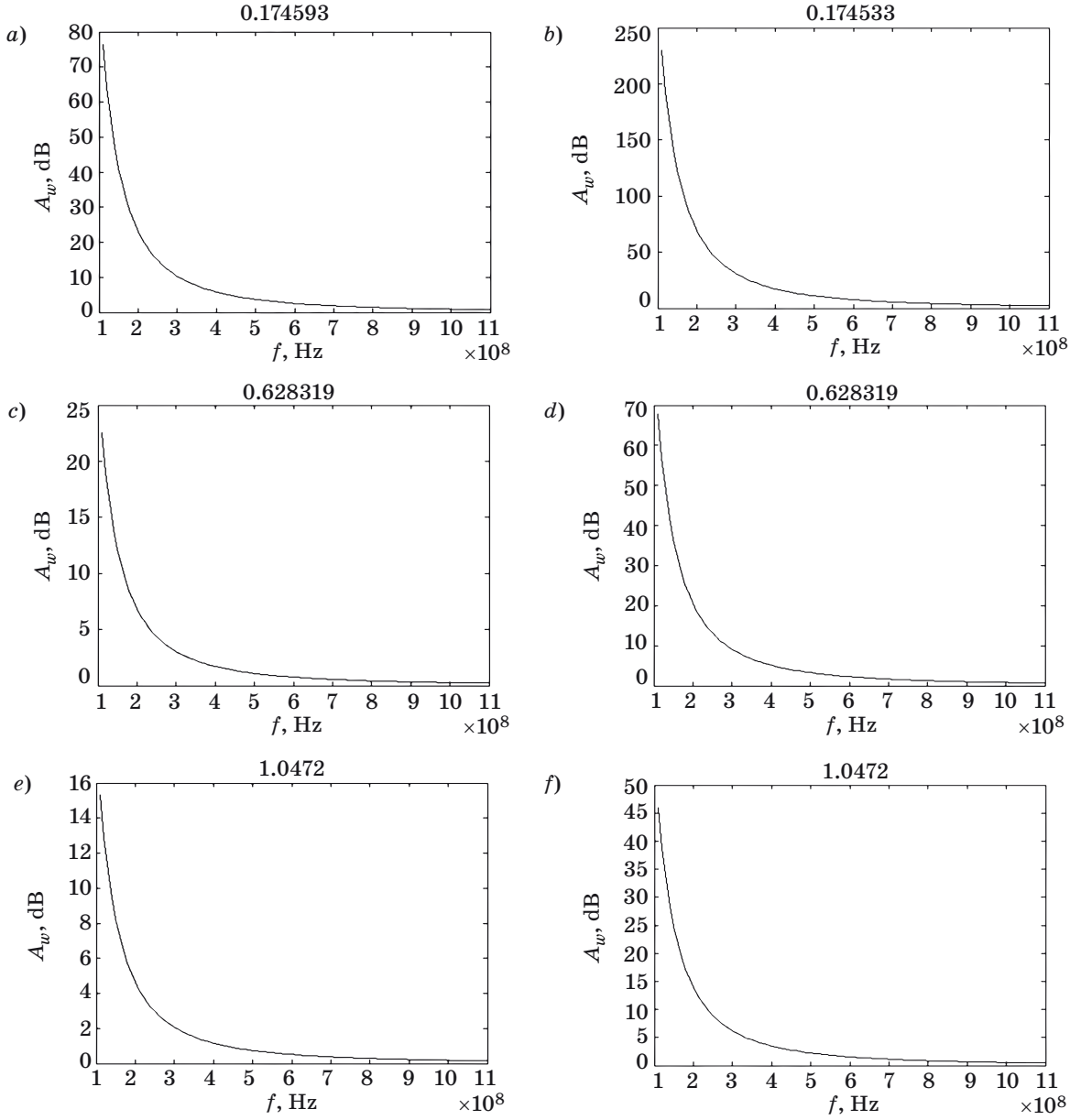

■ ***Fig. 4.*** Absorption of signal vs. frequency for weak magnetic storm (*a*, *c*, *e*) and strong magnetic storm (corresponding to Alaska region) (*b*, *d*, *f*): *a*, *b* — grazing angle $\psi \approx 0.175$ rad ($\psi \approx 10°$); *c*, *d* — $\psi \approx 0.628$ rad ($\psi \approx 36°$); *e*, *f* — $\psi \approx 1.05$ rad ($\psi \approx 60°$)

where ν_{em}, ν_{ei} and ν_{ee} are the frequencies of electron-neutral, electron-ion and electron-electron collisions, respectively.

The parameter of absorption fully characterizes real ionospheric radio traces and can usually be estimated by measuring radiometric absorption at the fixed frequencies and by knowledge of frequency dependence of coefficient of absorption κ. We should note that in integrand of (4) we account not only for the effects of electron-neutral and electron-ion collisions, but also ion-neutral and electron-electron collisions, based on the elements of kinetic theory [37–40], but not a magneto-ioning theory usually used in such computations based on hydrodynamic classical approach.

Then, accounting in (4) for the fact that the length of radio path, s, and the height of the ionosphere, h, are related as $h = s\sin\psi$, where ψ is the grazing angle of the satellite antenna with respect to the ground-based antenna, we can estimate the total absorption of radio signal along the radiopath. In Figs. 4, *a*–*f* this parameter is presented in [dB] vs. the carrier frequency of probing radio signal sent via stormtime ionosphere under different grazing angles, respectively. The corresponding profile of disturbed plasma density $N(h)$ is taken from Fig. 2 and normalized on the non-disturbed plasma density $N_0(h)$ taken from [15, 21] for the mid-latitude regular ionosphere, and accounting in computations of integral (4) for the limits $h_{\min} = 50$ km and $h_{\max} = 500$ km. We consider below two scenarios, weak and the strong magnetic storm, which are shown in Figs. 4, *a*, *c*, *e* and 4, *b*, *d*, *f* respectively. The corresponding data were taken from observations of magnetic storm, described above for weak storms observed at the middle latitude ionosphere above USA and at the northern regions of USA and Alaska.

As follows from above illustrations, with increase of the magnetic storm strength, from weak to strong, absorption of radio signals increases roughly three times at lower frequencies from 100 to 500 MHz, while at 500–600 MHz, absorption does not depend on frequency; only on the grazing angle. At the same time, with increase of the grazing angle, the tendency of decrease of signal absorption for week storms compared with strong storms is the same, per twice or three times. Results of computations presented above allow us to conclude that magnetic storms occurring in the northern mid-latitude ionosphere can significantly perturb ionospheric plasma and thus cause a dramatic attenuation of radio signals up to 500 MHz. This effect depends on the grazing angle and can be insignificant for grazing angles bigger than $\psi \geq 20°$. Hence with increase of the radiated frequency of radio signal for the same grazing angle or for increase of grazing angle for the same frequency, the tendency of significant decrease of signal energy absorption is evident.

Signal Point-to-Point Amplitude Attenuation and Phase Deviations

At the same time, we should point out that for radar and radio communication applications, other characteristics of signal fading can give information about radiophysical effects, dealing not with the cumulative intensity integral absorption along the radiopath, but with the point-to-point amplitude and phase deviations of the signal along the radiopath. In this case, it is important to understand of how perturbed parameters of the ionospheric plasma attenuate radio wave amplitude and change its phase. To understand these radiophysical effects, we will consider an arbitrary monochromatic radio wave [15]:

$$U(z, t) = A(z, t)\exp[j(\omega t - kz)]. \qquad (5)$$

In this case, the wave number k can be described through the coefficient of wave amplitude attenuation, α, and the coefficient determining changes of wave phase in real time, β, i.e.,

$$k = \alpha + j\beta. \qquad (6)$$

Unlike usual description of parameters α and β, we will present them through collision frequencies of plasma particles using elements of kinetic theory (see [15, 21]). For numerical computations, we introduce the additional notations and parameters to describe α and β, that is, $X = \omega_p^2 / \omega^2$, $Z = \nu/\omega$, ω_p is the background plasma density in the perturbed ionosphere [15, 37–39]. In these notations, after straightforward derivations, we obtained that

$$k^2 = \frac{\omega^2}{c^2}\left[1 - \frac{X}{1 - iZ}\right] = \frac{\omega^2}{c^2}\left[1 - \frac{X(1 + iZ)}{1 + Z^2}\right] = \frac{\omega^2}{c^2}\left[1 - \frac{X + iZX)}{1 + Z^2}\right] \qquad (7a)$$

or

$$k^2 = \frac{\omega^2}{c^2}\left[1 - \frac{X}{1 + Z^2} - i\frac{ZX}{1 + Z^2}\right]. \qquad (7b)$$

By introducing now normalized parameters (to the wave number in free space k_0), $\tilde{\alpha} = \frac{\alpha}{k_0}$ and $\tilde{\beta} = \frac{\beta}{k_0}$, we finally get:

$$\tilde{\alpha} = \frac{1 + \left(\frac{\nu}{\omega}\right)^2 - \frac{\omega_p^2}{\omega^2}}{1 + \left(\frac{\nu}{\omega}\right)^2} = \frac{\omega^2 + \nu^2 - \omega_p^2}{\omega^2 + \nu^2}; \qquad (8a)$$

$$\tilde{\beta} = \frac{ZX}{1+Z^2} = \frac{\left(\frac{\nu}{\omega}\right)\frac{\omega_p^2}{\omega^2}}{1+\left(\frac{\nu}{\omega}\right)^2} = \frac{\nu\omega_p^2}{\omega(\omega^2+\nu^2)}. \quad (8b)$$

Here $\nu = \nu_{em} + \nu_{ei} + \nu_{ee} = \nu_{em}(1 + q + q')$, where $q = \nu_{ei}/\nu_{em}$ and $q' = \nu_{ee}/\nu_{em}$.

Deviations of radio signal parameters, α and β, in the perturbed ionospheric region, were found by using parameters of the disturbed ionosphere, i. e., variations in the plasma frequency ω_p/ω_{p0}, plasma concentration N/N_0 ($N = N_0 + \delta N$, $\delta N < N_0$), and plasma conductivity σ/σ_0, where ω_{p0}, N_0, and σ_0 are the background non-disturbed ionospheric parameters [15, 21]

$$\omega_{p0} = (4\pi N_0 e^2/m_e)^{1/2}; \quad (9)$$

$$\varepsilon_0 = 1 - \left[\omega_0^2 / \left(\omega^2 + (\nu_{em} + \nu_{ei})^2\right)\right]; \quad (10)$$

$$\sigma_0 = \left[\omega_0^2(\nu_{em} + \nu_{ei}) / 4\pi\left(\omega^2 + (\nu_{em} + \nu_{ei})^2\right)\right]. \quad (11)$$

Here e and m_e are the charge and mass of plasma electron; other parameters are defined above.

Thus, in Fig. 5, *a*, *b* we present deviations of radio signal parameters, α and β, compared with those, α_0 and β_0, obtained for non-disturbed background ionospheric plasma. The computation results are shown in Fig 5, *a* (for normalized attenuation) and Fig. 5, *b* (for normalized phase velocity) versus altitude of the ionosphere for different frequencies of probing waves varied from 50 MHz to 2 GHz (i.e., covering also HF-bandwidth which is important for transionospheric propagation). Thus, we use

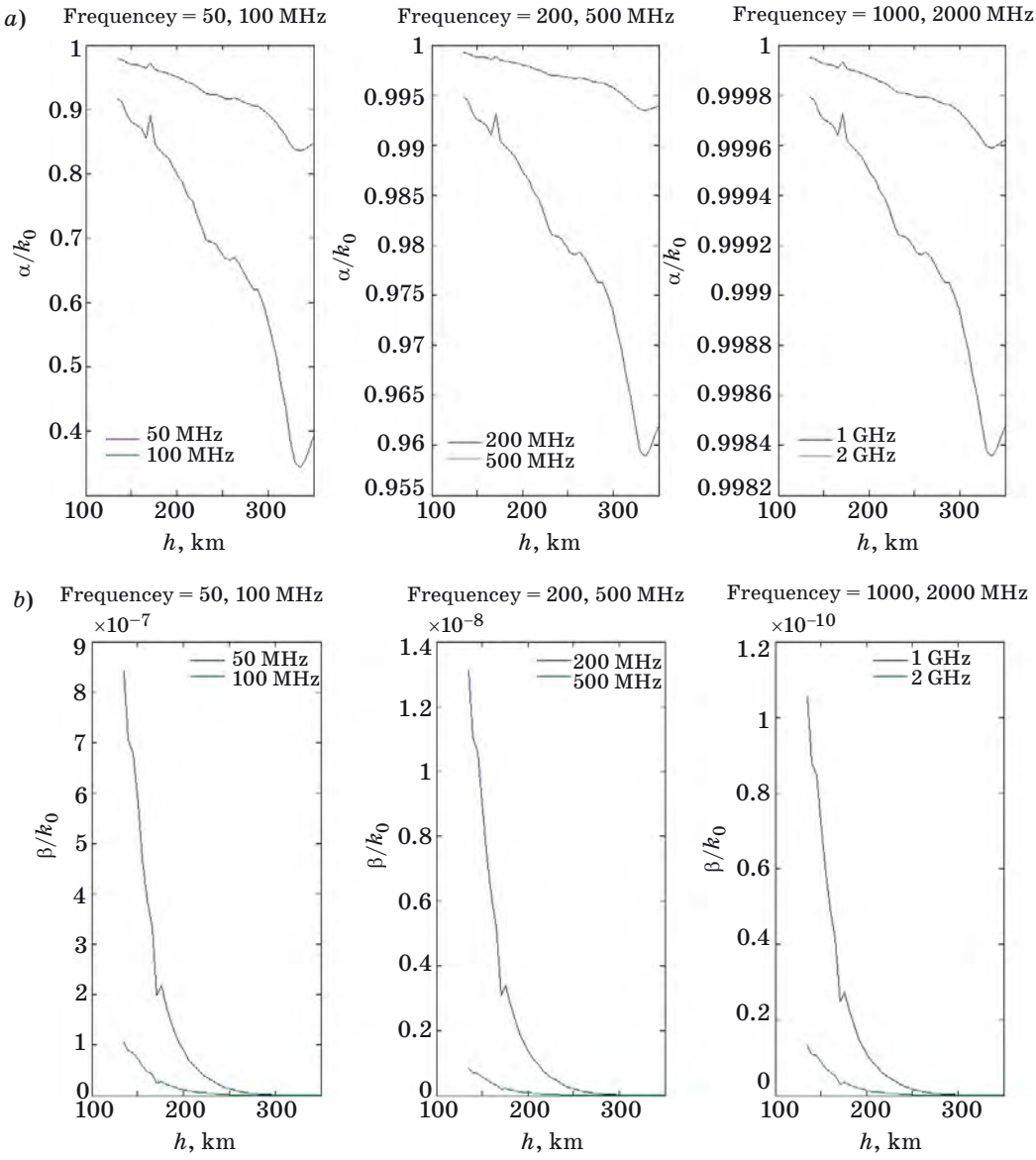

■ ***Fig. 5.*** Normalized attenuation coefficient (*a*) and phase velocity (*b*) of probing wave vs. ionospheric altitudes for frequencies varied from 50 MHz to 2 GHz

those frequencies which are actual both in land-ionosphere-land navigation ($f < 500$–600 MHz) and those which usually used in GPS radio monitoring of the ionosphere ($f > 900$ MHz).

As is seen from Fig. 5, *a* with the increase of frequency of the probing wave, the effect of attenuation of the wave energy becomes weaker, and the probing radio wave propagates at the same manner as in the non-disturbed ionosphere. This effect depends strongly on what altitudes the propagation process is observed. Thus, with increase of ionospheric altitude, attenuation affects stronger for all frequencies under consideration.

The same tendency of decreasing phase velocity of radio wave passing the disturbed ionospheric region with increase of frequency of probing wave is clear seen from Fig. 5, *b*. In fact, with increase of frequency from 50 MHz to 2 GHz, the normalized phase velocity, β/β_0, becomes smaller, i. e., the phase velocity of the probing wave becomes smaller in disturbed plasma compared with that in non-disturbed plasma.

This effect can be easily explained. When the frequency increases (or the wavelength decreases compared to the dimensions of plasma irregularities), the effects of "diffractive scattering" become weaker and, instead of defocusing with strong fading, we observe focusing with weak fading [15, 21].

Signal Intensity Fluctuations

To investigate the signal intensity deviations in the perturbed ionosphere and the corresponding scintillation index evaluations, the plane-screen [16–20, 23, 33, 34] and curved-screen ionospheric model [26, 27, 39] were performed and then summarized in [15]. Based on the theoretical self-consistent framework described there, one can estimate the effects of magnetic storm on the above two parameters of the radio signal propagating in perturbed ionospheric communication channel. Therefore, dealing only with situation occurring during magnetic storm described by the following PSD parameter $p = 4$ ($p' = 2$) introduced in first Section (see Fig. 3), we finally get, following [15, 21]

$$I(k) = 32\left\langle(\Delta\Phi)^2\right\rangle \frac{L_0}{(1+k^2L_0^2)^2}\sin^2\left(\frac{1}{2}k^2d_F^2\right). \quad (12)$$

Accounting for self-consistent theoretical framework described in [15, 21] for various scenarios occurring in the strongly perturbed ionosphere, we get for $p' = 2$ ($p = 4$) the following expression of the scintillation index:

$$\sigma_I^2 = \frac{8\sqrt{2}}{3\sqrt{\pi}L_0^3}d_F^3\left\langle(\Delta\Phi)^2\right\rangle. \quad (13)$$

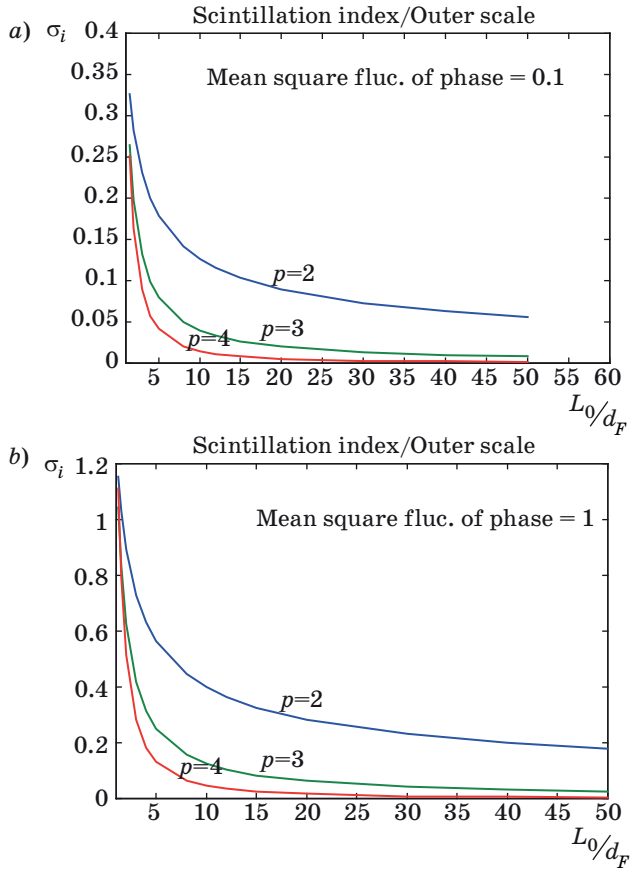

■ ***Fig. 6***. The RMS of the scintillation index, σ_I, vs. the outer scale L_0 for $1.5d_F \le L_0 \le 50d_F$, $\sqrt{\left\langle(\Delta\Phi)^2\right\rangle} = 0.1$ rad (*a*) and $\sqrt{\left\langle(\Delta\Phi)^2\right\rangle} = 1$ rad (*b*)

Computations of the scintillation index presented by (13) were compared in [15, 21] with those formulas obtained in [16–20, 23] for weak and moderate plasma perturbations [e. g., for $p = 2$ ($p' = 0$) and $p = 3$ ($p' = 1$), respectively], for an outer scale $L_0 = 10d_F$ and inner scale $l_0 = 10^{-2}d_F$. Figures 6, *a* and 6, *b* present the RMS of the scintillation index, $\sigma_I \equiv \sqrt{\sigma_I^2}$, computed for weak $\left(\sqrt{\left\langle(\Delta\Phi)^2\right\rangle} = 0.1 \text{ rad}\right)$ and moderate $\left(\sqrt{\left\langle(\Delta\Phi)^2\right\rangle} = 1 \text{ rad}\right)$ signal phase fluctuations versus square mean deviations of signal phase for various PSD parameters $p = 2$, 3, 4 and different scales of ionospheric irregularities.

It is seen that for $p = 2$ the scintillation index with increase of phase fluctuations limits to the unit. In the last case, for more higher spectral index ($p > 2$) σ_I exceeds the unit within the range of $0 < L_0/d_F < 1$, which explain us the focusing properties of the ionospheric layer consisting various irregularities and strong variations of signal phase after passing the perturbed ionosphere.

Signal Phase Deviations

We model the ionospheric *F*-region, according to [15, 21, 27], as a spherical 3-D layer of mean ionization density N and with the outer scale L_0 (instead of a plane-layer 1-D model, as was performed in [16–20, 24, 29–34]) with the standard fluctuations of ionization density, $(\Delta N/N_0)^2 \equiv (\delta N/N_0)^2$. We take the outer scale L_0 eqauals H, assuming latter as the thickness of the disturbed ionospheric *F*-layer. In such notations, the mean square fluctuation of phase of radio signal can be derived with the help of the general model [15, 21, 27], which finally gives:

$$\left\langle (\Delta\Phi)^2 \right\rangle = 4r_e^2 N_0^2 \left\langle \left(\frac{\delta N}{N_0} \right)^2 \right\rangle \lambda^2 H^2 \sec\chi. \qquad (14)$$

Here r_e is the radius of electron. For numerical computations we take $H = 100$ km and $N_0 = 10^{11}$ m^{-3}. In Figs. 7, *a* and *b* the RMS of the signal phase fluctuations, $\sqrt{\left\langle (\Delta\Phi)^2 \right\rangle}$, [in radian], are shown versus the zenith angle of a satellite for various frequencies from 32 MHz (HF-band) to 60 GHz (UHF-band) and for different $\delta N/N_0$ in percentages to the total plasma content of $N_0 = 10^{11}$ m^{-3}, from 1 % (weak magnetic storm) to 10 % (strong magnetic storm), respectively.

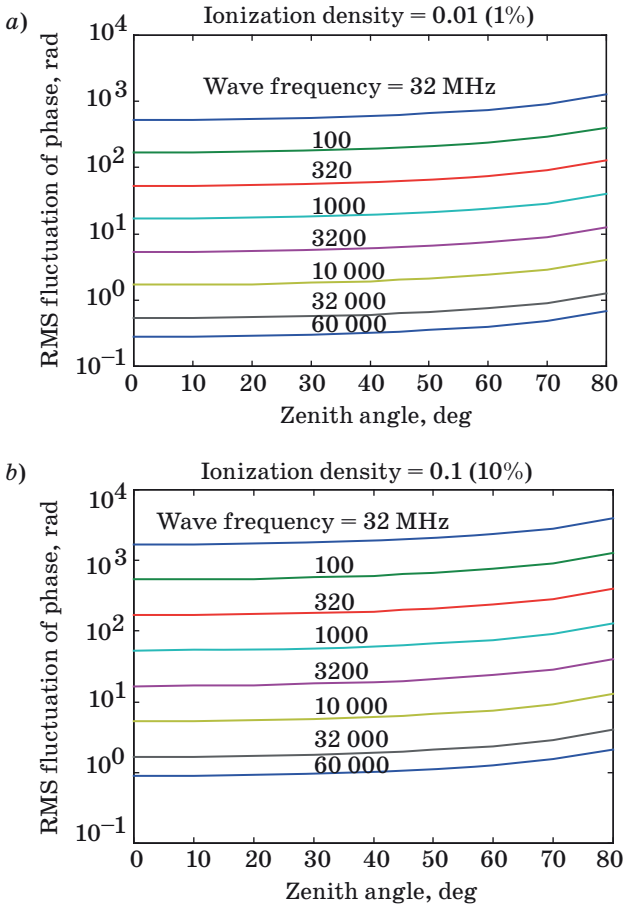

■ ***Fig. 7.*** RMS of signal phase fluctuation vs. zenith angle, for $\delta N/N_0 = 0.01$ (*a*) and for $\delta N/N_0 = 0.1$ (*b*) and for frequencies varied from 32 MHz to 60 GHz

Here, we should mention that the frequency band of signals that we investigate covers whole spectra of useful frequencies operating in existing land-ionosphere-land communication links, GPS satellite links and also in new networks beyond 3-G (third generation), operating at frequencies of 10 GHz to 60 GHz. As is clearly seen from the illustrations presented, the frequency dependence of RMS fluctuations of the signal phase is sufficient only for zenith angles greater 60–65° for mean and large perturbations of the background ionospheric plasma, i. e. 1 to 10 %. With increase of the radiated frequency, the phase fluctuations become strongly depending on $\delta N/N_0$. Thus, for the frequency band from 1 to 10 GHz usually used in satellite communications, for zenith angles of 50–60°, the RMS of phase fluctuations increases from 1–5 rad ($\delta N/N_0 = 0.1$ %) to 20 rad ($\delta N/N_0 = 1$ %) and 100 rad ($\delta N/N_0 = 10$ %).

Effects of Fast Fading on the Radio Signal

Based now on the magnetic storm effects experimentally observed during sounding of the disturbed stormtime ionosphere, we will analyze the effects of fading of radio signals determined by the *K*-factor of fading, defined above in Section “Main Parameters of the Radio Channel”.

For these purposes, we will use relations between the parameter of signal intensity scintillations σ_I^2 and the *K*-factor described by formula (3), as parameter of fast fading phenomena within the channel [15, 21]. Taking into account variations of scintillation parameter, $S_4 \equiv \sigma_I^2$, observed experimentally in [1, 2], from 0.4 to 0.8 (see also Figs. 1, 2), we get that the corresponding *K*-parameter varies in the range of 1.1 to 1.6, indicating the existence of direct visibility between the ground-based and satellite antenna. In the above cases the LOS component is at the same order or higher than the NLOS component.

In other words, the coherent component of signal intensity is accompanied by additional effects of multipath phenomena (i. e., by the incoherent component) caused by diffractive scattering of radio signals on small- and moderate-scale plasma density irregularities $\delta N/N_0$, which exist in stormtime ionosphere (see Figs. 1–3). This implies that the coherent (LOS) component exceeds the incoherent (NLOS) component even in stormtime perturbed ionospheric links. As was shown in [15, 21], knowing the *K*-factor of fast fading, one can predict deviations of the signal data passing through the disturbed ionospheric radio channel.

Conclusions

In this work, we presented theoretical predictions of the signal intensity and phase fluctuations of radio signals propagating in the stormtime subauroral ionosphere. The background ionospheric parameters and density irregularities used in the calculations are taken from the DMSP satellite observations during several magnetic storms that include two events where coincident intense radio-signal scintillations were observed (see first Section and the corresponding bibliography in [1–9]).

Based on experimental observations carried out in [1–9] and summarized in [21], as well as on theoretical framework developed in [15–20, 23–27, 31–34], the following phenomena can be predicted using these results.

1. *Deviation of plasma density*: weak storm — $\delta n / n_0 = 2 \div 5\%$; strong storm — $\delta n / n_0 = 10 \div 20\%$.

2. *Attenuation of signal amplitude*: the change is 3 times from weak to strong magnetic storm (see Fig. 4); the tendency which does not depend on grazing angle. With decrease of grazing angle, for frequencies up to 600 MHz, the attenuation of radio signal increases.

3. *Signal phase fluctuations*: from tens to hundreds radian from weak to strong magnetic storm (see Fig. 3).

4. *Scintillation index deviations*: from 0.4 to 0.8 (for $p = 2$) with respect to the non-perturbed ionosphere (see Fig. 6).

5. *Effect of fast fading*: $K \in [0.8 \div 1.6]$; I_{co} is at the same order or slightly higher then I_{inco}; the Ricean law can be used for description of such radio channels.

Finally, the knowledge of the main parameters of land-satellite communication links passing through the perturbed stormtime ionosphere allows estimates the main parameters of signal data, such as the capacity, spectral efficiency, and bit error rate. These aspects needs additional serious theoretical analysis and will be investigated in future.

References

1. Kintner P., and B. Ledvina. The Ionosphere, Radio Navigation, and Global Navigation Satellite Systems. *Adv. Space Res.*, 2005, vol. 35, pp. 788–811.
2. Basu Su., et al. Ionospheric Effects of Major Magnetic Storms During the International Space Weather Period of September and October 1999: GPS Observations, VHF/UHF Scintillations and in Situ Density Structures at Middle and Equatorial Latitudes. *J. Geophys. Res.*, 2001, vol. 106, pp. 389–399.
3. Ledvina B. M., Makela J. J., and Kitner P. M. First Observations of Intense GPS L1 Amplitude Scintillations at Midlatitude. *Geophys. Res. Lett.*, 2002, vol. 29, pp. 1659–1662.
4. Erickson P., Foster J., Holt and J. Inferred Electric Field Variability in the Polarization Jet from Millstone Hill E Region Coherent Scatter Radar Observations. *Radio Sci.*, 2002, vol. 37, iss. 2, pp. 1027–1036. doi:10.1029/2000RS002531
5. Mishin E., Burke W., Huang C., and Rich F. Electromagnetic Wave Structures Within Subauroral Polarization Streams. *J. Geophys. Res.*, 2003, vol. 108, pp. 1309–1315.
6. Mishin E., Burke W., and Viggiano A. Stormtime Subauroral Density Troughs: Ion-Molecule Kinetics Effects. *J. Geophys. Res.*, 2004, vol. 109, A10301. doi :10.1029/2004JA010438
7. Mishin E. V., and Burke W. J. Stormtime Coupling of the Ring Current, Plasmasphere and Topside Ionosphere: Electromagnetic and Plasma Disturbances. *J. Geophys. Res.*, 2005, vol. 110, pp. 7209–7216, A07209.
8. Foster J., and Burke W. A New Categorization for Subauroral Electric Fields. *EOS Trans. AGU*, 2002, vol. 83, pp. 393–401.
9. Mishin E., and Blaunstein N. Irregularities Within Subauroral Polarization Stream-Related Troughs and GPS Radio Interference at Midlatitudes. In: *Midlatitude Ionospheric Dynamics and Disturbances* (eds. P. Kintner, A. Coster, T. Fuller-Rowell, A. Mannucci, M. Mendillo, and R. Heelis). American Geophysical Union, Washington, D. C., 2008. Pp. 291–295. doi:10.1029/181GM26
10. Foster J., and Rich F. Prompt Midlatitude Electric Field Effects During Severe Magnetic Storms. *J. Geophys. Res.*, 1998, vol. 103, pp. 26367–26373.
11. Hardy D., Schmidt L., Gussenhoven M., Marshall F., Yeh H., Shumaker T., Huber A., and Pantazis J. Precipitating Electron and Ion Detectors (SSJ/4) for Block 5D/Flights 4-10 DMSP Satellites: Calibration and Data Presentation. *Tech. Rep., AFGL-TR-84-0317*, Air Force Geophys. Lab., Hanscom Air Force Base, Mass., 1984.
12. Maynard N., Burke W., Basinska E., Erickson G., Hughes W., Singer H., Yahnin A., Hardy D., and Mozer F. Dynamics of the Inner Magnetosphere Near Times of Substorm Onsets. *J. Geophys. Res.*, 1996, vol. 101, pp. 7705–7715.
13. Rich F. J., and Hairston M. Large-scale Convection Patterns Observed by DMSP. *J. Geophys. Res.*, 1994. vol. 79, pp. 3827–3835.
14. Saunders S. R. *Antennas and Propagation for Wireless Communication Systems*. New York, John Wiley & Sons, 1999. P. 409.
15. Blaunstein N., and Christodoulou Ch. G. *Radio Propagation and Adaptive Antennas for Wireless Communication Networks: Terrestrial, Atmospheric and Ionospheric*. Ed. 2. John Wiley & Sons, 2014. 704 p.
16. Booker H. G., and Gordon W. E. A Theory of Radio Scattering in the Ionosphere. *Proc. IRE*, 1950, vol. 38, pp. 400–412.

17. Booker H. G., Rateliffe S. A., and Shinn D. H. Diffraction from an Irregular Screen with Applications to Ionospheric Problems. *Philos. Trans. Roy. Soc. London*, *Ser. A*., 1950, vol. 242, pp. 579–607.
18. Booker H. G. A Theory of Scattering by Non-isotropic Irregularities with Application to Radar Reflection from the Aurora. *J. Atmos. Terr. Phys*., 1956, vol. 8, pp. 204–221.
19. Booker H. G., and Majidi Ahi G. Theory of Refractive Scattering in Scintillation Phenomena. *J. Atmos. Terr. Phys*., 1981, vol. 43, pp. 1199–1214.
20. Booker H. G. Application of Refractive Scintillation Theory to Radio Transmission through the Ionosphere and the Solar wind and to Reflection from a Rough Ocean. *J. Atmos. Terr. Phys*., 1981, vol. 43, pp. 1215–1233.
21. Blaunstein N., and Plohotniuc E. *Ionosphere and Applied Aspects of Radio Communication and Radar*. London-New York, CRC Press, 2008. 599 p.
22. Blaunstein N., and Christodoulou Ch. *Radio Propagation and Adaptive Antennas for Wireless Communication Links*: *Terrestrial, Atmospheric and Ionospheric*. Wiley & Sons, 2007. 614 p.
23. Farley D. T. Incoherent Scatter Radar Probing. In: *Modern Ionospheric Science*. Ed. by H. Kohl, R. Ruster, and K. Schlegel. Katlenburg-Lindau, Copernicus GmbH, 1996. Pp. 415–439.
24. Denisov N. G., and Erukhimov L. M. Statistical Properties of Phase Fluctuations During Total Reflection from a Layer. *Geomagn. and Aeronomy*, 1966, vol. 5, pp. 695–702.
25. Erukhimov L. M., and Rizhkov V. A. Study of Focusing Ionospheric Irregularities by Methods of Radio-Astronomy at Frequencies of 13–54 MHz. *Geomagn. and Aeronomy*, 1971, vol. 5, pp. 693–697.
26. Erukhimov L. M., Komrakov G. P., and Frolov V. L. About the Spectrum of the Artificial Small-Scale Ionospheric Turbulence. *Geomagn. and Aeronomy*, 1980, vol. 20, pp. 1112–1114.
27. Gajlit T. A., Gusev V. D., Erukhimov L. M., and Shpiro P. I. Spectrum of the Phase Fluctuations at the Ionosphere Sounding. *Izvestija vuzov. Radiofizika*, 1983, vol. 26, no. 7, pp. 795–801 (In Russian).
28. Backley R. Diffraction by Random Phase Screen with Very Large RMS Phase Deviation. Two-dimensional screen. *Austral. J. Phys*., 1971, vol. 24, pp. 373–396.
29. Titheridge J. E. The Diffraction of Satellite Signals by Isolated Ionospheric Irregularities. *J. Atmos. Terr. Phys*., 1971, vol. 33, pp. 47–69.
30. Crain C. M., Booker H. G., and Fergusson S. A. Use of Refractive Scattering to Explain SHF Scintillations. *Radio Sci*., 1974, vol. 14, pp. 125–133.
31. Wernik A. W., and Liu C. H. Application of the Scintillation Theory to Ionospheric Irregularities Studies. *J. Artificial Satellites*, 1975, vol. 10, pp. 37–58.
32. Rino C. L., and Fremouw E. J. The Angle Dependence of Single Scattered Wave Fields. *J. Atmos. Terr. Phys*., 1977, vol. 39, pp. 859–868.
33. Knepp D. L. Multiple Phase-Screen Calculation of the Temporal Behavior of Stochastic Waves. *Proc. IEEE*, 1983, vol. 71, pp. 722–737.
34. Rino C. L. On the Application of Phase Screen Models to the Interpretation of Ionospheric Scintillation Data. *Radio Sci*., 1982, vol. 17, pp. 855–867.
35. Gurevich A. V., and Tsedilina E. E. *Sverkhdal'nee rasprostranenie korotkikh radiovoln* [Long-Range Propagation of Short Waves]. Moscow, Nauka Publ., 1979. 344 p. (In Russian).
36. Burke W., Rubin A., Mayanard M., et al. Ionospheric Disturbances Observed by DMSP at Mid to low Latitudes During Magnetic Storm of June 4–6, 1991. *J. Geophys. Res*., 2000, vol. 105, pp. 18391–19402. doi:10.1029/1999JA000188
37. Shkarofsky I. P., Johnston T. W., and Bachynski M. P. *The Particle Kinetics of Plasmas*. London, Addison-Wesley, 1966. 518 p.
38. Gurevich A. V. *Nonlinear Phenomena in the Ionosphere*. Berlin, Springer-Verlag, 1978. 465 p.
39. Gel'berg M. G. *Neodnorodnosti vysokoshirotnoi ionosfery* [Inhomogeneities of High-Latitude Ionosphere]. Novosibirsk, Nauka Publ., 1986. 193 p. (In Russian).
40. Silin V. P. *Vvedenie v kineticheskuiu teoriiu gazov* [Introduction in the Kinetic Theory of Gases]. Moscow, Nauka Publ., 1971. 332 p. (In Russian).

УДК 654.165
doi:10.15217/issn1684-8853.2018.1.85

Прогнозирование эксплуатационных параметров прохождения радиосигналов в канале «Земля — спутник» через возмущенную ионосферу

Блаунштейн Н. Ш.[a], доктор физ.-мат. наук, профессор, nathan.blaunstein@hotmail.com
Бен-Шимол И.[a], PhD, техн., старший преподаватель, benshimo@bgu.ac.il
[a]Негевский университет им. Бен-Гуриона, П.О.Б. 653, Бен-Гуриона ул., 1, г. Беэр-Шева, 74105, Израиль

Введение: тема исследования стала актуальной в последнее время ввиду глобализации систем беспроводной связи за счет использования дальнего ионосферного распространения радиоволн в каналах связи «Земля — спутник». **Цель:** анализ ключевых параметров ультракоротких радиоволн в канале «Земля — спутник», которые определяют эффекты фединга при магнитных бурях, происходящих в среднеширотной ионосфере. **Результат:** при возмущенных параметрах плазмы, вызванных экспериментально магнитным штормом, проанализированы поглощение и фазовые флуктуации радиосигналов. На основе экспериментальных дан-

ных исследован индекс сцинтилляции σ_I^2, соответствующий сцинтилляциям сигналов в многолучевых каналах связи с федингом. Показано, что ~10 % нерегулярностей плотности плазмы во время шторма в области *F* вызывают сильный фединг высокочастотных радиосигналов диапазона ультракоротких радиоволн со значительными флуктуациями интенсивности сигнала (до 1 %) и изменениями фазы сигнала (до сотен радиан). **Практическая значимость:** полученные результаты позволяют прогнозировать мультипликативный фединг в ионосферных субканалах и его вклад в определение потерь в полном канале связи «Земля — спутник».

Ключевые слова — ионосферный субканал, ионосферные нерегулярности плотности плазмы, индекс сцинтилляции интенсивности сигнала, затухание амплитуды, флуктуации фазы, среднеквадратическая величина, радиоволны УКВ-диапазона.

Цитирование: Blaunstein N., Ben-Shimol Y. Prediction of Operational Parameters of Radio Signals Passing a Land-Satellite Link through StormTime Ionosphere // Информационно-управляющие системы. 2018. № 1. С. 85–95. doi:10.15217/issn1684-8853.2018.1.85
Citation: Blaunstein N., Ben-Shimol Y. Prediction of Operational Parameters of Radio Signals Passing a Land-Satellite Link through StormTime Ionosphere. *Informatsionno-upravliaiushchie sistemy* [Information and Control Systems], 2018, no. 1, pp. 85–95. doi:10.15217/issn1684-8853.2018.1.85

Уважаемые авторы!

При подготовке рукописей статей необходимо руководствоваться следующими рекомендациями.

Статьи должны содержать изложение новых научных результатов. Название статьи должно быть кратким, но информативным. В названии недопустимо использование сокращений, кроме самых общепринятых (РАН, РФ, САПР и т. п.).

Объем статьи (текст, таблицы, иллюстрации и библиография) не должен превышать эквивалента в 20 страниц, напечатанных на бумаге формата А4 на одной стороне через 1,5 интервала Word шрифтом Times New Roman размером 13, поля не менее двух сантиметров.

Обязательными элементами оформления статьи являются: индекс УДК, заглавие, инициалы и фамилия автора (авторов), ученая степень, звание (при отсутствии — должность), полное название организации, аннотация и ключевые слова на русском и английском языках, электронные адреса авторов, которые по требованию ВАК должны быть опубликованы на страницах журнала. При написании аннотации не используйте аббревиатур и не делайте ссылок на источники в списке литературы.

Статьи авторов, не имеющих ученой степени, рекомендуется публиковать в соавторстве с научным руководителем, наличие подписи научного руководителя на рукописи обязательно; в случае самостоятельной публикации обязательно предоставляйте заверенную по месту работы рекомендацию научного руководителя с указанием его фамилии, имени, отчества, места работы, должности, ученого звания, ученой степени — эта информация будет опубликована в ссылке на первой странице.

Формулы набирайте в Word, не используя формульный редактор (Mathtype или Equation), при необходимости можно использовать формульный редактор; для набора одной формулы не используйте два редактора; при наборе формул в формульном редакторе знаки препинания, ограничивающие формулу, набирайте вместе с формулой; для установки размера шрифта никогда не пользуйтесь вкладкой Other…, используйте заводские установки редактора, не подгоняйте размер символов в формулах под размер шрифта в тексте статьи, не растягивайте и не сжимайте мышью формулы, вставленные в текст; в формулах не отделяйте пробелами знаки: + = –.

Для набора формул в Word никогда не используйте Конструктор (на верхней панели: «Работа с формулами» — «Конструктор»), так как этот ресурс предназначен только для внутреннего использования в Word и не поддерживается программами, предназначенными для изготовления оригинал-макета журнала.

При наборе символов в тексте помните, что символы, обозначаемые латинскими буквами, набираются светлым курсивом, русскими и греческими — светлым прямым, векторы и матрицы — прямым полужирным шрифтом.

Иллюстрации предоставляются отдельными исходными файлами, поддающимися редактированию:

— рисунки, графики, диаграммы, блок-схемы предоставляйте в виде отдельных исходных файлов, поддающихся редактированию, используя векторные программы: Visio 4, 5, 2002-2003 (*.vsd); Coreldraw (*.cdr); Excel (*.xls); Word (*.doc); AdobeIllustrator (*.ai); AutoCad (*.dxf); Matlab (*.ps, *.pdf или экспорт в формат *.ai);

— если редактор, в котором Вы изготавливаете рисунок, не позволяет сохранить в векторном формате, используйте функцию экспорта (только по отношению к исходному рисунку), например, в формат *.ai, *.esp, *.wmf, *.emf, *.svg;

— фото и растровые — в формате *.tif, *.png с максимальным разрешением (не менее 300 pixels/inch).

Наличие подрисуночных подписей обязательно (желательно не повторяющих дословно комментарии к рисункам в тексте статьи).

В редакцию предоставляются:

— сведения об авторе (фамилия, имя, отчество, место работы, должность, ученое звание, учебное заведение и год его окончания, ученая степень и год защиты диссертации, область научных интересов, количество научных публикаций, домашний и служебный адреса и телефоны, e-mail), фото авторов: анфас, в темной одежде на белом фоне, должны быть видны плечи и грудь, высокая степень четкости изображения без теней и отблесков на лице, фото можно представить в электронном виде в формате *.tif, *.png с максимальным разрешением — не менее 300 pixels/inch при минимальном размере фото 40×55 мм;

— экспертное заключение.

Список литературы составляется по порядку ссылок в тексте и оформляется следующим образом:

— для книг и сборников — фамилия и инициалы авторов, полное название книги (сборника), город, издательство, год, общее количество страниц;

— для журнальных статей — фамилия и инициалы авторов, полное название статьи, название журнала, год издания, номер журнала, номера страниц;

— ссылки на иностранную литературу следует давать на языке оригинала без сокращений;

— при использовании web-материалов указывайте адрес сайта и дату обращения.

Список литературы оформляйте двумя отдельными блоками по образцам lit.dot на сайте журнала (http://i-us.ru/paperrules) по разным стандартам: Литература — СИБИД РФ, References — один из мировых стандартов.

Более подробно правила подготовки текста с образцами изложены на нашем сайте в разделе «Оформление статей».

Контакты
Куда: 190000, Санкт-Петербург,
Б. Морская ул., д. 67, ГУАП, РИЦ
Кому: Редакция журнала «Информационно-управляющие системы»
Тел.: (812) 494-70-02
Эл. почта: ius.spb@gmail.com
Сайт: www.i-us.ru